JOURNAL OF BACTERIOLOGY, Aug. 2004, p. 5450–5459 Vol. 186, No. 16
0021-9193/04/$08.00+0 DOI: 10.1128/JB.186.16.5450–5459.2004

spoIVH (*ykvV*), a Requisite Cortex Formation Gene, Is Expressed in Both Sporulating Compartments of *Bacillus subtilis*

Daisuke Imamura,[1] Kazuo Kobayashi,[2] Junichi Sekiguchi,[3] Naotake Ogasawara,[2] Michio Takeuchi,[1] and Tsutomu Sato[1]*

International Environmental and Agricultural Science, Tokyo University of Agriculture and Technology, Fuchu, Tokyo 183-8509,[1] Graduate School of Information Science, Nara Institute of Sciences and Technology, Ikoma, Nara 630-0101,[2] and Department of Applied Biology, Faculty of Textile Science and Technology, Shinshu University, Ueda, Nagano 386-8567,[3] Japan

Received 27 January 2004/Accepted 18 May 2004

It is well known that the *ykvU-ykvV* operon is under the regulation of the σ^E-associated RNA polymerase ($E\sigma^E$). In our study, we observed that *ykvV* is transcribed together with the upstream *ykvU* gene by $E\sigma^E$ in the mother cell and monocistronically under $E\sigma^G$ control in the forespore. Interestingly, alternatively expressed *ykvV* in either the forespore or the mother cell increased the sporulation efficiency in the *ykvV* background. Studies show that the YkvV protein is a member of the thioredoxin superfamily and also contains a putative Sec-type secretion signal at the N terminus. We observed efficient sporulation in a mutant strain obtained by replacing the putative signal peptide of YkvV with the secretion signal sequence of SleB, indicating that the putative signal sequence is essential for spore formation. These results suggest that YkvV is capable of being transported by the putative Sec-type signal sequence into the space between the double membranes surrounding the forespore. The ability of *ykvV* expression in either compartment to complement is indeed intriguing and further introduces a new dimension to the genetics of *B. subtilis* spore formation. Furthermore, electron microscopic observation revealed a defective cortex in the *ykvV* disruptant. In addition, the expression levels of σ^K-directed genes significantly decreased despite normal σ^G activity in the *ykvV* mutant. However, immunoblotting with the anti-σ^K antibody showed that pro-σ^K was normally processed in the *ykvV* mutant, indicating that YkvV plays an important role in cortex formation, consistent with recent reports. We therefore propose that *ykvV* should be renamed *spoIVH*.

The gram-positive bacterium *Bacillus subtilis* forms dormant and environmentally resistant spores in response to nutrient deprivation (10). Early in sporulation, cells divide into two unequal compartments, a larger mother cell and a smaller forespore (24, 34). Just after septation, RNA polymerase sigma factors σ^F and σ^E govern gene expressions in the forespore and in the mother cell, respectively (14, 19). Later in sporulation, after the completion of the engulfment of the forespore by the mother cell, σ^G and σ^K become activated and replace σ^F and σ^E in the forespore and mother cell compartments, respectively (23, 25, 42). Prior to the completion of the engulfment process, an inactive precursor protein pro-σ^K, which contains an N-terminal extension of 20 amino acids (aa), is produced in the mother cell (6, 20, 26). The processing of pro-σ^K into an active form requires the expression of the signaling protein SpoIVB in the forespore under the control of σ^G (4, 46). A processing complex consisting of SpoIVFA, SpoIVFB, and BofA receives the signal via SpoIVB that engulfment is completed, and then pro-σ^K is processed into active σ^K in the mother cell (5, 27, 36). The engulfment process culminates in two bilayer membranes surrounding the forespore. A thick peptidoglycan layer is then deposited between the two membranes of the forespore to form the spore cortex that confers heat resistance on the spore (13). The coordinated functions of this cascade of sigma factors ensure distinct regulation of hundreds of sporulation-specific genes, including many whose functions are not yet known.

With the successful completion of the *B. subtilis* genome-wide sequence (21), the current focus of the *B. subtilis* functional genomics project is to identify the roles of all genes of unknown functions by gene disruption with insertional mutagenesis and pMUTIN vectors (31). Within the framework of this project, the sporulation-deficient *spoIVH* mutant was identified.

Recently, Eichenberger et al. (8) and Feucht et al. (11) reported that *spoIVH* is required for efficient sporulation and is transcribed from the consensus sequence of the σ^E-recognized promoter located upstream of *ykvU*. In this paper, we report that *spoIVH* is expressed in both compartments under the control of σ^E and σ^G. This is the first instance of nonspecific compartment expression of a sporulation gene during spore formation in *B. subtilis*.

MATERIALS AND METHODS

Measurement of sporulation frequencies. Sporulation efficiency was measured by incubating *B. subtilis* cells in DSM (Difco sporulation medium) (39) at 37°C for 24 h. The number of spores per milliliter of culture (CFU) was determined as the number of heat-resistant (80°C for 10 min) colonies on tryptose blood agar base.

Plasmid and strain constructions. Table 1 lists the bacterial strains and plasmids used in this study. *B. subtilis* was transformed and plasmids were constructed in *Escherichia coli* JM105 by standard methods (7, 37).

Integration plasmids pJMVU and pJMIVH were constructed as follows. PCR-amplified products were generated. The 237-bp internal segment of *ykvU* was generated with primers ykvU-F (5′-CCGGAATTCTATGATTTTGGCGCGG

* Corresponding author. Mailing address: International Environmental and Agricultural Science, Tokyo University of Agriculture and Technology, Fuchu, Tokyo 183-8509, Japan. Phone and fax: 81 423 67 5706. E-mail: subtilis@cc.tuat.ac.jp.

TABLE 1. Bacterial strains and plasmids used in this study

Strain or plasmid	Genotype and/or relevant characteristics	Source, reference, or construction[a]
E. coli JM105	*supE endA sbcB15 hsdR4 rpsL thi* Δ(*lac-proAB*)F′ [*traD36 proAB*$^+$ *lacI*^{q} *lacZ*ΔM15]	47
B. subtilis		
168	*trpC2*	Laboratory stock
YKVVd	*trpC2 spoIVH*::pMUTIN2MCS	31
YKVUd	*trpC2 ykvU*::pMUTIN2MCS	31
TS001	*trpC2 spoIVH*::pJMIVH	This study
TS002	*trpC2 ykvU*::pJMVU	This study
SSPEd	*trpC2 sspE*::pMUTIN2MCS	31
RL13	spβ::*gerE-lacZ*	R. Losick
REZ	*trpC2* spβ::*gerE-lacZ*	RL13 → 168
PE6	*amyE*::*spoIIE-gus*::*cat thr*::pCW63(*cotD-lacZ*)::*erm divIB*::*spc*	R. Losick
TDZ	*trpC2 thr*::pCW63(*cotD-lacZ*)::*erm*	PE6 → 168
TS003	*trpC2 spoIVH*::pJMIVH *sspE*::pMUTIN2MCS	TS001 → SSPEd
TS004	*trpC2 spoIVH*::pJMIVH spβ::*gerE-lacZ*	TS001 → REZ
TS005	*trpC2 spoIVH*::pJMIVH *thr*::pCW63(*cotD-lacZ*)::*erm*	TS001 → TDZ
TS006	*trpC2 thrC*::pTCE10(*spoIVH*)	This study
TS007	*trpC2 thrC*::pTCE11(P_{spoIVH}-*spoIVH*)	This study
TS008	*trpC2 thrC*::pTCE12(P_{ykvU}-*spoIVH*)	This study
TS009	*trpC2 thrC*::pTCE13(P_{sspE}-*spoIVH*)	This study
TS010	*trpC2 spoIVH*::pJMIVH *thrC*::pTCE10	TS006 → TS001
TS011	*trpC2 spoIVH*::pJMIVH *thrC*::pTCE11	TS007 → TS001
TS012	*trpC2 spoIVH*::pJMIVH *thrC*::pTCE12	TS008 → TS001
TS013	*trpC2 spoIVH*::pJMIVH *thrC*::pTCE13	TS009 → TS001
TS014	*trpC2 thrC*::pTCE14(P_{spoIVH}-*spoIVH*Δsignal)	This study
TS015	*trpC2 thrC*::pTCE15(P_{sleB}-$signal_{sleB}$-*spoIVH*Δsignal)	This study
TS016	*trpC2 spoIVH*::pJMIVH *thrC*::pTCE14	TS014 → TS001
TS017	*trpC2 spoIVH*::pJMIVH *thrC*::pTCE15	TS015 → TS001
TF97	*trpC2 spo0A*::*cat*	K. Kobayashi
TF85	*trpC2 sigH*::*cat*	K. Kobayashi
TF83	*trpC2 sigF*::*cat*	K. Kobayashi
TF82	*trpC2 sigE*::*cat*	K. Kobayashi
TF84	*trpC2 sigG*::*cat*	K. Kobayashi
TF99	*trpC2 spoIIIC*::*cat*	K. Kobayashi
Plasmids		
pMUTIN2MCS	Vector carrying *bla erm*	31
pJM114	Vector carrying *bla kan*	33
pHY300PLK	Vector carrying *bla tet*	18
pCBB31	Vector carrying *bla cat*	38
pTCC0	pCBB31 carrying a *thrC* 5′ region	This study
pTCC1	Integration vector at *thrC* carrying *bla* and *cat*	This study
pUC18	Vector carrying *bla*	43
pUC19	Vector carrying *bla*	47
pE194	Vector carrying *erm*	16
pTC1	Vector carrying *bla*	This study
pTC2	Vector carrying *bla erm*	This study
pTC3	Vector carrying *bla erm*	This study
pTCE1	Integration vector at *thrC* carrying *bla* and *erm*	This study
pJMVU	pJM114 carrying an internal region of *ykvU*	This study
pJMIVH	pJM114 carrying an internal region of *spoIVH*	This study
pTCE10	pTCE1 carrying *spoIVH*	This study
pTCE11	pTCE1 carrying P_{spoIVH}-*spoIVH*	This study
pTCE12	pTCE1 carrying P_{ykvU}-*spoIVH*	This study
pTCE13	pTCE1 carrying P_{sspE}-*spoIVH*	This study
pTCE14	pTCE1 carrying P_{spoIVH}-*spoIVH*Δsignal	This study
pTCE15	pTCE1 carrying P_{sleB}-$signal_{sleB}$-*spoIVH*+79Δsignal	This study

[a] Arrows indicate transformation from the donor DNA to the recipient strain.

G-3′, the EcoRI site is underlined) and ykvU-R (5′-CGCGGATCCGGAATA AACGGAAGCGC-3′, the BamHI site is underlined), and the 168-bp internal segment of *spoIVH* was generated with primers IVH-F (5′-CCGGAATTCCTG CTGTTCCCGCTGTT-3′, the EcoRI site is underlined) and IVH-R (5′-CGCG GATCCCACTGTCGGATGGATGG-3′, the BamHI site is underlined). These products were trimmed with the respective restriction enzymes and then ligated with pJM114 (33) digested with EcoRI/BamHI. The resulting plasmids, pJMVU and pJMIVH, were used to transform competent cells of *B. subtilis* 168 to generate strains TS002 and TS001, respectively.

To obtain the vector pTCE1 to enable the introduction of DNA fragments into the *thrC* region by double crossover, a 993-bp 5′ region and a 990-bp 3′ region of the *thrC* gene were amplified with primer pairs thrC-UF (5′-CGGGGTACC TTGAAGCCAGTGTTGCC-3′, the KpnI site is underlined) and thrC-UR (5′-CGCGGATCCTGTAAAGTTAGCGCCGG-3′, the BamHI site is underlined)

and thrC-DF (5′-AAAACTGCAGGAAATCACCGATTGCCC-3′, the PstI site is underlined) and thrC-DR (5′-CCCAAGCTTGTCCGCTTCAGACAGCT-3′, the HindIII site is underlined), respectively. The plasmid that was used, pCBB31 (38), harbors a Cm^r cassette flanked by unique KpnI/BamHI and PstI/HindIII sites. The 993-bp PCR product was trimmed with the enzymes KpnI and BamHI and then ligated with pCBB31 digested with KpnI/BamHI, resulting in the plasmid pTCC0. The 990-bp product was cut with PstI and HindIII and then ligated with pTCC0 digested with PstI/HindIII, resulting in the plasmid pTCC1. Next, the multiple cloning sequence region of pHY300PLK (18) was digested with EcoRI and HindIII, and the small 39-bp fragment was ligated into pUC19 (47) to obtain plasmid pTC1. A 1,197-bp HpaII and BanIII fragment of the *erm* gene from pE194 (16) was cloned into the AccI site of pTC1 to generate plasmid pTC2. To obtain plasmid pTC3, a 1,218-bp BamHI and XbaI fragment of the *erm* gene of pTC2 was cloned into the BamHI and XbaI site of pUC18 (43). A 1,213-bp BamHI and BglII fragment of the *erm* gene of pTC3 was cloned into the BamHI and BglII site of pTCC1, resulting in a BamHI- and BglII-digestible plasmid named pTCE1.

To obtain the plasmids pTCE10 and pTCE11, which harbor the SpoIVH coding region with and without promoter, respectively, DNA segments of positions −115 to +515 and −28 to +515 relative to the *spoIVH* start codon were amplified from strain 168 chromosomal DNA with primers IVH-115X (5′-TGCTCTAGAGCAAAGCATTGAAGGTA-3′, the XbaI site is underlined) or IVH-28X (5′-TGCTCTAGACTAATTGAAAAGCATGA-3′, the XbaI site is underlined) each against primer IVH-RB (5′-CGCGGATCCAGAGTCTATGCTCTCAG-3′, the BamHI site is underlined), respectively. These PCR products were trimmed with the respective restriction enzymes and then ligated with XbaI/BglII-digested pTCE1. The resulting plasmids, pTCE10 and pTCE11, were linearized with ScaI and then used for the introduction of *spoIVH* (without promoter) and P$_{spoIVH}$-*spoIVH* into the *thrC* locus of *B. subtilis* strain 168 through a double-crossover event. Erythromycin-resistant transformants were selected to obtain strains TS007 and TS006 with and without *spoIVH* promoter, respectively.

For plasmids pTCE12 and pTCE13, which harbor the SpoIVH coding region plus the *ykvU* (σ^E) or *sspE* (σ^G) promoter region, respectively, the DNA segment containing positions −28 to +515 of the *spoIVH* region was amplified with IVH-28H (5′-CCCAAGCTTCTAATTGAAAAGCATGA-3′, the HindIII site is underlined) and IVH-RB, and then the promoter regions of *ykvU* (positions −113 to −13 from the initiation codon of the *ykvU* gene) and *sspE* (positions −58 to −12 from the initiation codon of the *sspE* gene) were amplified with primers ykvU-113 (5′-TGCTCTAGAATTTGTCTCAGCTGTGC-3′, the XbaI site is underlined) and ykvU-13 (5′-CCCAAGCTTTGTCTCTTGTACTACCA-3′, the HindIII site is underlined) and primers sspE-58 (5′-TGCTCTAGAAAAGAGGAATAGCTAT-3′, the XbaI site is underlined) and sspE-12 (5′-CCCAAGCTTCCACGGTCATTAGAATG-3′, the HindIII site is underlined), respectively. These PCR products were trimmed with the respective restriction enzymes and then ligated with XbaI/BglII-digested pTCE1.

For plasmid pTCE14 with the putative P$_{spoIVH}$ promoter plus the signal sequence-less SpoIVH coding region, the DNA segment from −115 to +3 of *spoIVH* and the DNA segment from +79 to +515 relative to the *spoIVH* start codon were amplified with the primer pairs IVH-115X and IVH-3H (5′-CCCAAGCTTCATGGAATCTTCCTTTC-3′, the HindIII site is underlined) and IVH-sig-H (5′-CCCAAGCTTGAGGAAAAACAGCCTGC-3′, the HindIII site is underlined) and IVH-RB, respectively. These PCR products were trimmed with the respective restriction enzymes and then ligated with pTCE1 digested with XbaI/BglII. Plasmid pTCE15, harboring the P$_{sleB}$ promoter to the *sleB* signal sequence coding region plus the signal sequence-less SpoIVH coding region, was constructed by amplifying the DNA segment from −79 to +87 of *sleB* and the DNA segment from +79 to +515 with primer pairs sleB-FX (5′-TGCTCTAGAAAGGAAAGAGTGTCTAA-3′, the XbaI site is underlined) and sleB-RH (5′-CCCAAGCTTGGCAGAGATCGTTTCAG-3′, the HindIII site is underlined) and IVH-sig-H and IVH-RB, respectively. These PCR products were trimmed with each restriction enzyme and then ligated with pTCE1 digested with XbaI/BglII to obtain the plasmid pTCE15.

Plasmids pTCE12, pTCE13, pTCE14, and pTCE15 were used for the introduction of P$_{ykvU}$-*spoIVH*, P$_{sspE}$-*spoIVH*, P$_{spoIVH}$-*spoIVH* Δsignal, and P$_{sleB}$-signal$_{sleB}$-*spoIVH* Δsignal into the *thrC* locus of *B. subtilis* strain 168 through a double-crossover event by selecting for erythromycin-resistant transformants to generate strains TS008, TS009, TS014, and TS015, respectively. Proper constructions were verified by PCR and DNA sequencing.

Electron microscopy. *B. subtilis* cells that were grown in casein growth medium at 37°C and induced to sporulate by the resuspension method for 6 h were collected by centrifugation. Transmission electron micrographs were taken at UltraStructure Research Laboratories (Kanagawa, Japan). Samples were prefixed in 2% (wt/vol) glutaraldehyde in 0.1 M phosphate buffer (pH 7.4), fixed with 1% osmic acid, and successively stained with 2% uranyl acetate. Epoxy Spurr resin (Okenshoji Co., Ltd) was used for embedding the cells. Sections (800 Å) of the cells were prepared with an LKB Co. U5 ultramicrotome (Amersham Pharmacia) and examined with a JEOL Co. JEM 100S electron microscope.

DPA quantification. The dipicolinic acid (DPA) content in sporulating cells was determined. At hourly intervals until 12 h after the end of log-phase growth (T_{12}) and then subsequently T_{24}, suspended cells and the culture medium were harvested by centrifugation (13,000 × *g*, 2 min) from 1.5 ml of culture. The pellet was resuspended in 1 ml of sterile distilled water, boiled for 20 min, cooled for 15 min on ice, and then separated by centrifugation at 9,000 × *g* for 2 min. The supernatant (600 μl) was reacted with 200 μl of 50 mM sodium acetate (25 ml, pH 4.6, adjusted with acetic acid) containing 25 mg of L-cysteine, 0.31 g of $FeSO_4 \cdot 7H_2O$, and 80 mg of $(NH_4)_2SO_4$. The DPA content was determined as the optical density at 440 nm (1).

β-Galactosidase assay. Activities of β-galactosidase were determined as described by Miller (28) with *o*-nitrophenyl-β-D-galactopyranoside as the substrate. Enzyme-specific activity is expressed as nanomoles of substrate (*o*-nitrophenyl-β-D-galactopyranoside) hydrolyzed per milligram per minute.

Immunoblot analysis. To detect pro-σ^K and σ^K by Western immunoblotting, *B. subtilis* cells were grown in casein growth medium at 37°C and induced to sporulate by the resuspension method (41). Protein samples were extracted from cultures taken at different time points. Samples were separated by sodium dodecyl sulfate-polyacrylamide gel electrophoresis and analyzed by Western immunoblotting with polyclonal anti-σ^K serum (12).

Northern hybridization. Samples of cultures in DSM at 37°C were drawn at intervals, and total RNA was extracted from harvested cells as described previously (17). Total RNA (5 μg) resolved by electrophoresis was blotted onto a positively charged nylon membrane (Hybond N$^+$; Amersham Pharmacia) and hybridized by using digoxigenin-labeled RNA probes (10 ng) according to the manufacturer's instructions (Roche). The following oligonucleotide primers were used to amplify the specific templates for probe generation: *ykvU*, ykvU-F2 (5′-AATGCCTTGAATTTGTCGTC-3′) and ykvU-T7R (5′-TAATACGACTCACTATAGGGCGAGAAATCAGCACAGCCATGTC-3′); *spoIVH*, IVH-F1 (5′-ATGTTGACGAAGCGCTTGC-3′) and IVH-T7R (5′-TAATACGACTCACTATAGGGCGACAATCGGAAACGTCAGCTTG-3′).

Primer extension. Cells were grown in DSM at 37°C and withdrawn at T_{-1}, T_3, and T_4. Total RNA was extracted from harvested cells as described previously (17). One hundred micrograms of total RNA and 1 pmol of the infrared-dye (IRD)-labeled oligonucleotide primer IVH-EX (5′-GCACCATGACGTCCAAAAATGGAG-3′), which is complementary to the nucleotide sequence of the *spoIVH* gene and the 3′ end of the primer located 172 nucleotides (nt) downstream from the initiation codon, were mixed and heated at 80°C for 15 min. Samples were incubated at 25°C for 10 min, and then reverse transcription reactions were carried out with 400 U of SuperScript III reverse transcriptase (Invitrogen) at 55°C for 60 min. Reactions were inactivated at 70°C for 15 min and treated with RNaseH. Ethanol-precipitated products were run on 5% polyacrylamide–6 M urea gels with a sequencing ladder. The DNA fragments amplified by PCR with IVH-115 and IVH-RB were sequenced with IVH-EX to generate a sequence ladder. IRD was detected with a LI-COR DNA sequencer model 4200 (Aloka).

Compartmental localization of β-galactosidase activity. Cells in 200 μl of cultures were sedimented by centrifugation and resuspended into 200 μl of 50 μM fluorescein di-β-D-galactopyranoside (FDG) substrate reagent (Marker Gene Technologies, Inc.). Samples were incubated for 2 min at 37°C, and then FDG loading was terminated by the addition of 900 μl of ice-cold phosphate-buffered saline buffer (100 ml, pH 7.6, containing 0.8 g of NaCl, 0.02 g of KCl, 0.29 g of $Na_2HPO_4 \cdot 12H_2O$, 0.02 g of KH_2PO_4, and 0.28 g of HEPES). Cells were placed on ice until examination by fluorescence microscopy (22).

Fluorescence microscopy. *B. subtilis* cells incubated in hydrolyzed casein growth medium at 37°C were induced to sporulate by the resuspension method of Sterlini and Mandelstam (41), as specified by Nicholson and Setlow (30) and Partridge et al. (32). The resuspension medium was supplemented with FM4-64 (final concentration, 0.5 μg/ml; Molecular Probes) for staining of the cell membranes. Samples mounted on glass slides coated with 0.1% poly-L-lysine (Sigma) were observed with an Olympus BX50 microscope with a 100× UplanApo objective. Images were captured by using a SenSys charge-coupled device camera (Photometrics). FM4-64 and FDG were visualized by using a wide interference green filter set (Olympus) or a fluorescein isothiocyanate filter set (Olympus) and processed by using Metamorph, version 4.5, software (Universal Image) and Adobe Photoshop, version 4.0.1J.

TABLE 2. Defective sporulation in *spoIVH* disruptant[a]

Strain	Description	No. (CFU/ml) of:		Frequency[b]
		Viable cells	Spores	
168	Wild type	4.7×10^8	3.4×10^8	0.72
TS001	*spoIVH*::pJMIVH	2.7×10^8	1.3×10^4	4.8×10^{-5}
TS002	*ykvU*::pJMVU	4.8×10^8	2.5×10^8	0.52

[a] Cells were grown in DSM.
[b] Frequency is the ratio of the number of spores to that of viable cells for each strain.

RESULTS

Disruption of *spoIVH* (*ykvV*) blocks stage IV of sporulation. The *ykvV* (named *spoIVH*) pMUTIN2MCS insertional mutant YKVVd was identified as a heat-sensitive spore phenotype during a screening of disruptants of genes of unknown function in *B. subtilis*. Consistent with a recent report (8), the *spoIVH* mutant TS001 sporulated in DSM at a low frequency of about 0.0001 (Table 2). The forespores were mostly phase dark (data not shown). We further examined the structure of the forespores by electron microscopy. After engulfment is completed, the cortex layer is synthesized at the inner space between double membranes surrounding the forespore in *B. subtilis*. The wild-type cortex was obvious as a white layer at T_6 (Fig. 1a). Although we observed more than 20 cells, the *spoIVH* mutant did not form a visible cortex layer (Fig. 1b and c), suggesting that the absence of SpoIVH may have some effects on spore cortex formation.

DPA accumulation significantly decreased in mutant spores. Several previous studies indicate that the accumulation of DPA is impaired in mutants with a defective cortex (1, 2). We therefore proceeded to examine the cortex integrity of the *spoIVH* mutant by quantifying the DPA content in pellets of centrifuged culture (Fig. 2). We observed significantly less DPA accumulation in the *spoIVH* mutant than in wild-type cells. Together, these results confirm defective cortex formation in *spoIVH* mutant spores. Based on these late-stage characteristics, we classified *ykvV* as a stage IV sporulation gene and renamed it *spoIVH*.

Effect of *spoIVH* mutation on the sigma cascade. To determine the effect of a *spoIVH* mutation on the activity of the sporulation-specific RNA polymerase sigma cascade comprising σ^F, σ^E, σ^G, and σ^K, we compared the expressions of various *lacZ* fusions in the presence or absence of an intact *spoIVH* gene. Although σ^F, σ^E, and σ^G activities were normal (Fig. 3A and data not shown), the expression of σ^K-directed *gerE-lacZ* and σ^K-directed GerE-dependent *cotD-lacZ* was inhibited (Fig. 3A). These results suggest that *spoIVH* mutation affects the sigma cascade after the activation of forespore-specific σ^G and partially shuts down mother cell-specific σ^K activation late in sporulation. The expression of low σ^K-directed genes and normal σ^F-, σ^E-, and σ^G-directed genes in the *spoIVH* mutant suggests that the *spoIVH* gene product is necessary for efficient pro-σ^K processing.

To examine this hypothesis, we Western blotted the *spoIVH* mutant with anti-σ^K antibody. Figure 3B shows that both the *spoIVH* mutant and the wild-type strain contained the mature form of σ^K from T_4 to T_6. Densitometry analysis showed that the levels of both pro-σ^K and σ^K observed in the wild type and the *spoIVH* mutant at every examined time point were not significantly different (data not shown). These results indicate that pro-σ^K processing is not impaired by *spoIVH* inactivation, suggesting that decreased activity of σ^K may result from an indirect effect of the *spoIVH* mutation, most probably caused by an abnormal condition in the mother cell resulting from impaired sporulation.

Transcriptional analysis of *spoIVH*. In a recent report, Eichenberger et al. (8) and Feucht et al. (11) indicated that *ykvU*, located upstream of *spoIVH* (Fig. 4A), and *spoIVH* were cotranscribed by Eσ^E by microarray analysis. In addition, Eichenberger et al. (8) identified a transcriptional start site of the *ykvU-spoIVH* operon and found a promoter very similar to the consensus sequence recognized by Eσ^E, 5′-Ata-16 bp-cATAcanT-3′ (15), in the −27 to −56 segment of *ykvU* (8). However, plasmid integration in *ykvU*, whose mutation is expected to prevent the expression of *spoIVH*, did not abolish the sporulation efficiency (Table 2). These findings indicate that there may be a promoter located just upstream of *spoIVH*. To investigate the transcription of the *ykvU* and *spoIVH* genes, we examined RNA synthesis by Northern blotting of RNA extracted from growing and sporulating cells (Fig. 4B). The *ykvU* gene probe detected a band at approximately 2.0 kb (band b, T_2 and T_3), corresponding to the predicted length of a transcript initiated at the *ykvU* promoter and terminating at the putative terminator located downstream of the *spoIVH* coding region. The *spoIVH* gene-specific probe detected bands of about 2.0 kb (T_2 to T_3), 0.5 kb (T_3 to T_7), and 0.4 kb (vegetative cells and T_0). The largest band corresponded to band b, which was detected with the *ykvU* probe. A smaller band (band c) corresponded to the predicted length of a transcript initiated

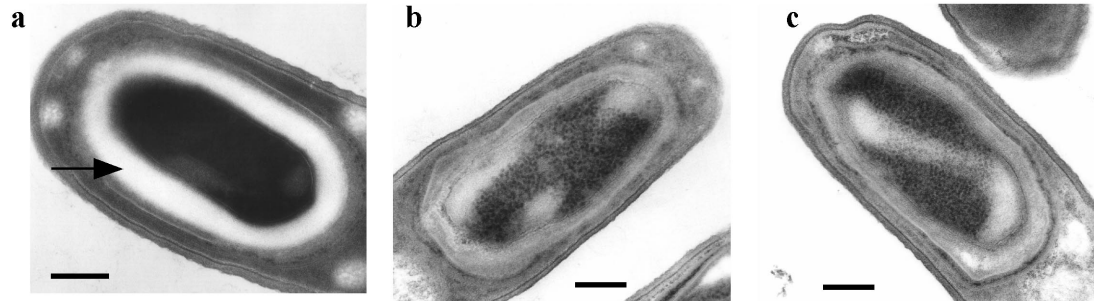

FIG. 1. Transmission electron micrographs of typical sporulating cells. Wild-type 168 (a) and *spoIVH* mutant TS001 (b and c) were allowed to sporulate for 6 h after the initiation of sporulation. The arrow indicates the wild-type cortex layer. Bar, 0.2 μm.

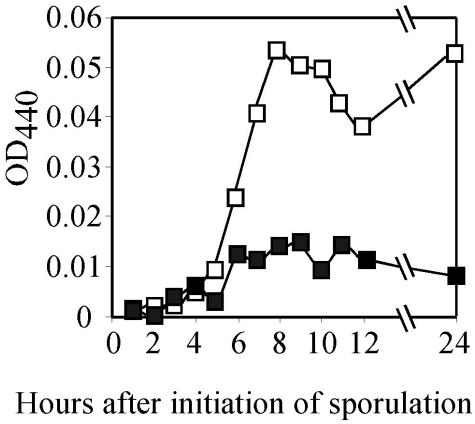

FIG. 2. Quantification of DPA. Cultures of 168 (□) and TS001 (■) were induced to sporulate in resuspension medium. Aliquots were withdrawn at the indicated time points. Time zero (0) corresponds to the initiation of sporulation. The optical density at 440 nm (OD_{440}) directly reflects the DPA concentration.

upstream of *spoIVH* and terminating in a stem and loop structure at the end of the *ykvU-spoIVH* transcriptional unit. The smallest band (band a), detected at the vegetative stage and at T_0, seems slightly shorter than band c and the *spoIVH* gene (498 bp). Probably, the band a signal is not specific for *spoIVH* mRNA. However, even if *spoIVH* is expressed in the vegetative phase and is functional, it may be one of several similar proteins including paralogous genes, so its inactivation had little or no effect on growth.

To determine the dependence of *spoIVH* expression, we analyzed transcripts from the two promoters that function in the sporulation phase at T_2 and T_4 in *spo0A* (Spo0A), *spo0H* (σ^H), *spoIIAC* (σ^F), *spoIIGB* (σ^E), *spoIIIG* (σ^G), and *spoIIIC* (σ^K) mutant backgrounds (Fig. 4C). A band (band b) was detected in the wild type and the *spoIIIG* and *spoIIIC* mutants but not in the *spo0A*, *spo0H*, *spoIIAC*, and *spoIIGB* mutants. The transcript (band c) was detected only in the wild type and in the *spoIIIC* mutant (Fig. 4C). These results indicate that *spoIVH* is transcribed together with *ykvU* from T_2 to T_3 by $E\sigma^E$ from the promoter located upstream of *ykvU*, consistent with previous reports (8, 11), and transcribed monocistronically from T_3 under $E\sigma^G$ control from promoter P_{spoIVH}, indicated in Fig. 4A.

To determine the 5′ end of *spoIVH* mRNA transcribed by $E\sigma^G$, we carried out the primer extension analysis with total RNA extracted from strain 168 (Fig. 5A). Although the transcription start site was not detected at the vegetative phase, it was located 23 to 25 nt upstream of the initiation codon of *spoIVH* at T_3 and T_4. Consistent with our results, we found a region highly similar to the consensus sequence recognized by σ^G, 5′-gnATA/G-18 bp-cAtnnTA-3′ (15), in the *spoIVH* segment from −27 to −56 from its initiation codon (Fig. 5B). An extension reaction was primed from 172 nt downstream of the initiation codon of *spoIVH* with IRD-labeled primer IVH-EX. However, a vegetative-phase-specific extension product was not detected (data not shown), suggesting that band a, detected as shown in Fig. 4B, may not be specific for *spoIVH* mRNA.

To confirm the compartment localization of *spoIVH* expression, we used fluorescence microscopy and the β-galactosidase

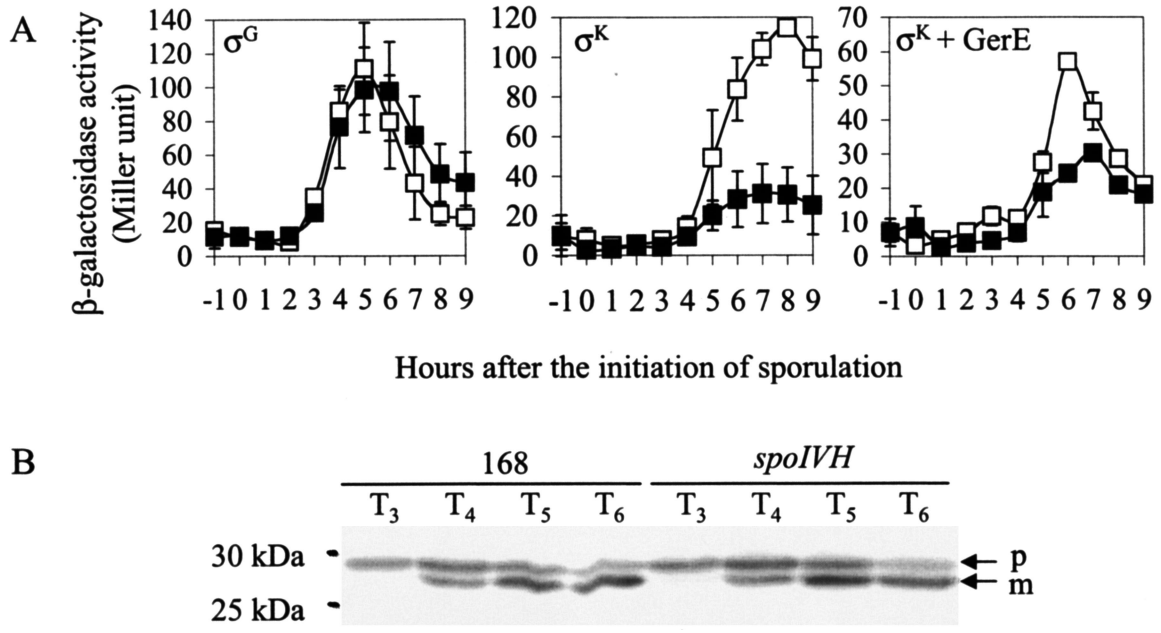

FIG. 3. Effects of *spoIVH* mutation on sigma cascade. Strains carrying *lacZ* fusions along with intact (□) or disrupted (■) *spoIVH* were induced to sporulate, and β-galactosidase activities were assayed. σ^G, σ^G-directed *sspE-lacZ* expression (□, SSPEd; ■, TS003). σ^K, σ^K-directed *gerE-lacZ* expression (□, REZ; ■, TS004). σ^K+GerE, σ^K-directed and GerE-dependent *cotD-lacZ* expression (□, TDZ; ■, TS005). Averages of the results from three or two independent experiments are shown. Error bars represent standard deviations. (B) Western blots of pro-σ^K processing in strain 168 and the *spoIVH* mutant (TS001). Cells were induced into sporulation and collected at the indicated time points. Whole-cell extracts were Western blotted with antibody that recognizes σ^K. p and m indicate pro-σ^K and mature σ^K, respectively.

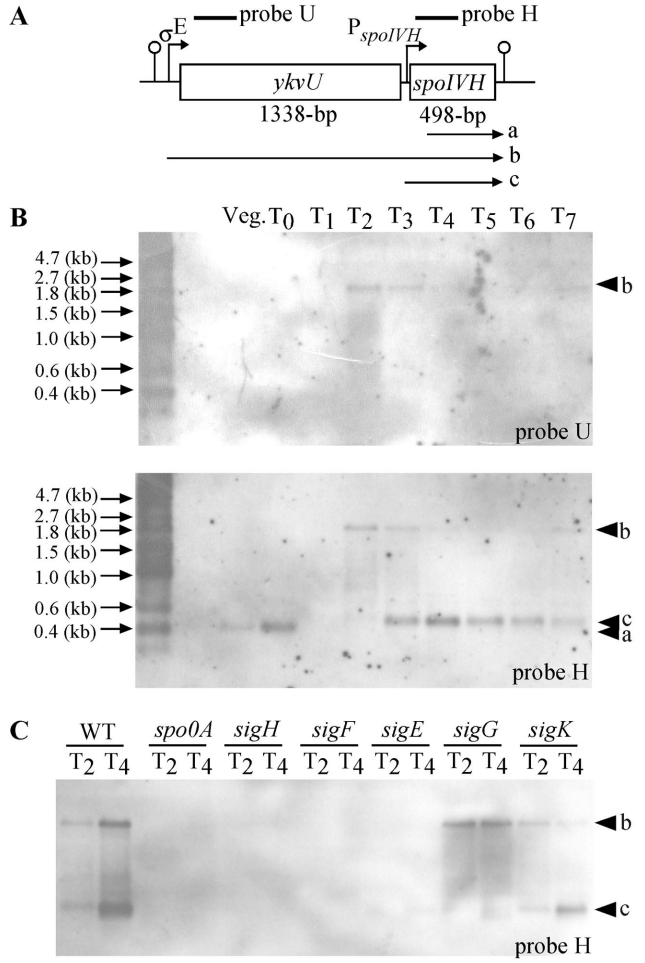

FIG. 4. Transcriptional analysis of *spoIVH* region. (A) Arrangement of *spoIVH* and upstream gene *ykvU*. Bars indicate the positions of sequences corresponding to the Northern blotting probe. Loops with lines indicate putative terminators. Arrows with lines indicate (putative) promoters. Arrows under the physical map indicate observed mRNA. (B) Northern blots of whole RNA extracted from wild-type 168 cells. Arrows indicate positions of molecular size markers. Cells were grown on DSM and harvested at the indicated time points. (C) Northern blot of whole RNA extracted from 168 with disruptions of the indicated genes. WT, 168; *spo0A*, TF97; *sigH*, TF85; *sigF*, TF83; *sigE*, TF82; *sigG*, TF84; *sigK*, TF99; arrowheads, mRNA signals; Veg., vegetative cells.

sensitive substrate FDG, which can show compartment expression of the *lacZ* gene (22). Fluorescence from FDG in *spoIID-lacZ* (σ^E) and *sspE-lacZ* (σ^G) strains was detected in the mother cell and in the forespore compartment, respectively (data not shown). No fluorescence from FDG was detected under our conditions in the wild-type strain (data not shown). In the *ykvU* and *spoIVH* insertional mutants with the pMUTIN2MCS vector, the *lacZ* gene was integrated into each of the genes, meaning β-galactosidase is expressed from the promoter for *ykvU* and *spoIVH*. Figure 6 shows that FDG fluorescence was detected in the mother cell at T_2 in both strains. At T_4, in the strain carrying *ykvU-lacZ* (YKVUd), fluorescence was still detectable in the mother cells (Fig. 6A) and in both compartments of the *ykvU-spoIVH-lacZ* (YKVVd) strain (Fig. 6B). Furthermore, the signal became more intense in the forespore than in the mother cell at T_6 in the *ykvU-spoIVH-lacZ* strain. The percentage of compartment expression in cells that showed FDG fluorescence is shown to the right of the pictures (Fig. 6). At least 377 cells were counted in each sample. In the *ykvU-lacZ* strain, although the number of cells showing FDG green fluorescence decreased from T_2 to T_6 (35, 22, and 17% of cells at T_2, T_4, and T_6, respectively), FDG fluorescence was observed only in the mother cell compartment at every observed time point. In contrast, *ykvU-spoIVH-lacZ* expression was detected only in the mother cell at T_2; however, it was observed in both compartments in 14 and 39% of cells at T_4 and T_6, respectively. In the *ykvU-spoIVH-lacZ* strain, FDG fluorescence was observed only in the forespore in 51% of cells at T_6. These results suggest that *ykvU* and *spoIVH* are expressed only in the mother cell early in sporulation; however, *spoIVH* alone is expressed in the forespore during late sporulation.

Alternative expression of *spoIVH*. To determine the essentiality of *spoIVH* expression in the forespore and mother cell for efficient sporulation, we constructed strains in which *spoIVH* is transcribed in the forespore only or in the mother cell only (Fig. 7). Although strain TS010, which has intact *spoIVH* without promoter, did not support wild-type levels of sporulation (frequency of 0.0017), the expression of *spoIVH* from the putative σ^G promoter located just upstream of *spoIVH* was completely sufficient for proper spore formation (0.81 in TS011), as shown in Table 3. This is consistent with the obser-

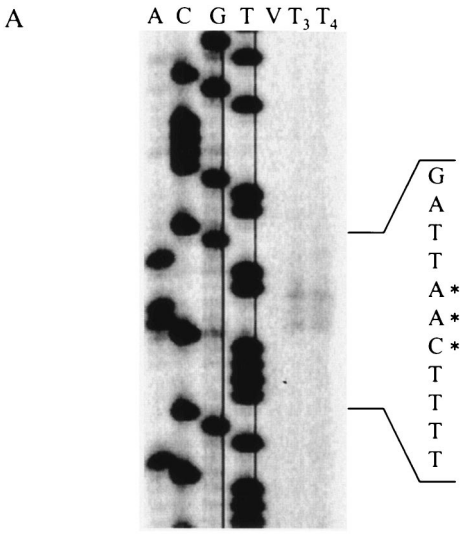

FIG. 5. Mapping of the transcription start sites of *spoIVH* by primer extension analysis. (A) Total RNA was prepared from wild-type 168 of exponentially growing cells (lane V) or at T_3 (lane T_3) or T_4 (lane T_4). (B) Nucleotide sequence of the upstream region of *spoIVH*. The regions with similar consensus sequences recognized by σ^G are underlined. The positions of primer-extended products are indicated with asterisks.

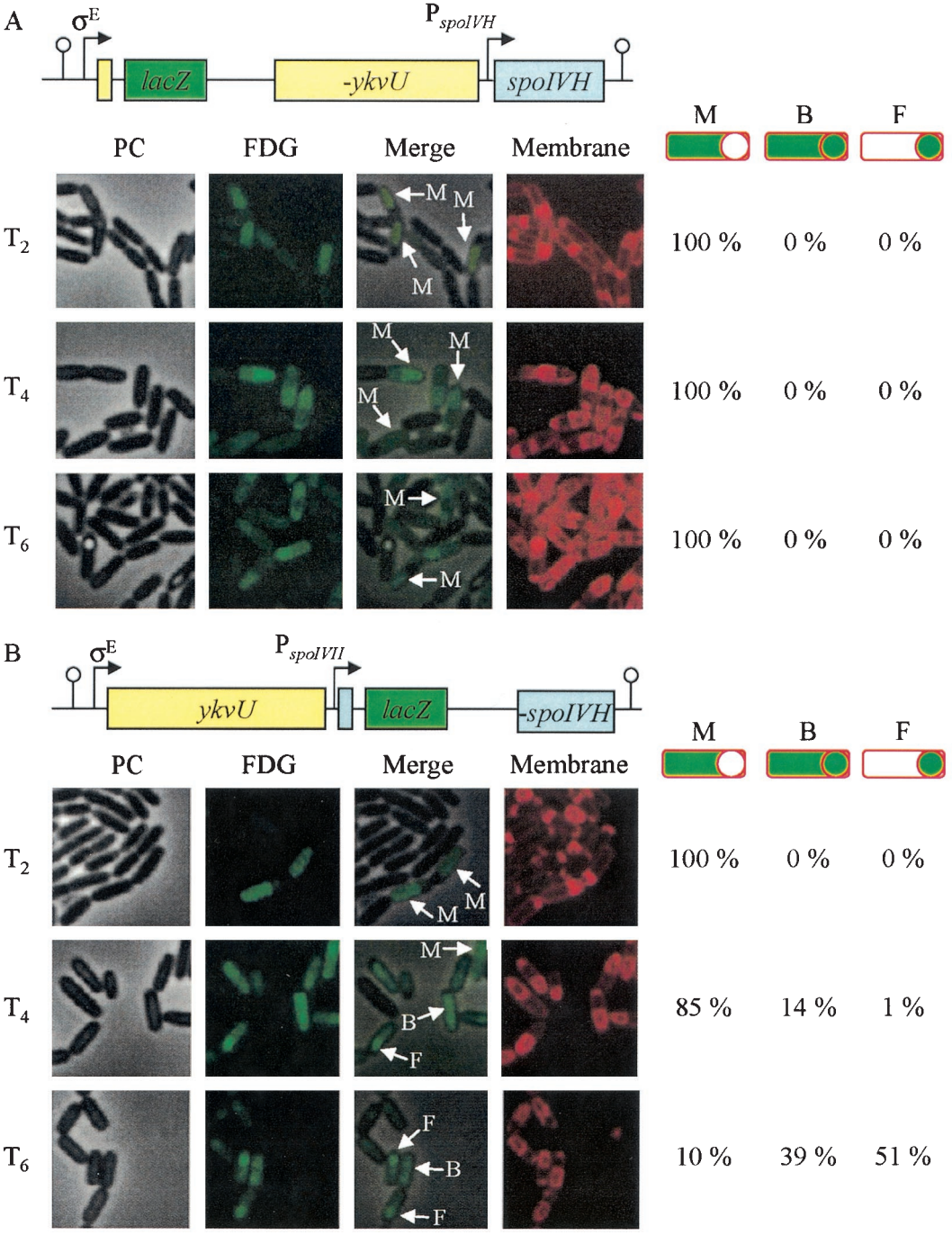

FIG. 6. Compartmental expression of *spoIVH*. Strains YKVUd (A) and YKVVd (B) were induced to sporulate, and after the indicated time, samples were prepared for fluorescence microscopy and stained with FDG. PC, phase contrast; FDG, FDG fluorescent signal; Merge, merge of PC and FDG; Membrane, FM4-64-stained membrane. Arrows indicate typical cells. M, F, and B indicate the cells in which the FDG signal was observed in the mother cell, forespore, and both compartments, respectively. Cells were induced to sporulation by the resuspension method and observed at the indicated time points. Ratios of compartmental expression are shown to the right of the pictures. At least 377 cells were counted at the indicated time points. This number did not include cells that showed no fluorescence.

vation that the *ykvU* insertional mutant sporulated normally. In the event of a polar effect, the transcription of *spoIVH* from *ykvU* may be blocked in the *ykvU* mutant and the expression of *spoIVH* would be effected only from its own promoter. Interestingly, the sporulation deficiency of the *spoIVH* mutant strain was compensated completely (0.94) or partially (0.13) by the introduction of the σ^G (P_{sspE}, TS013)- and σ^E (P_{ykvU}, TS012)-directed *spoIVH* genes, respectively (Table 3). These results suggest that *spoIVH* is capable of contributing to spore formation from both sporulating cell compartments. It is, however, quite puzzling how *spoIVH* functions from both compartments.

We could not detect SpoIVH localization by using the

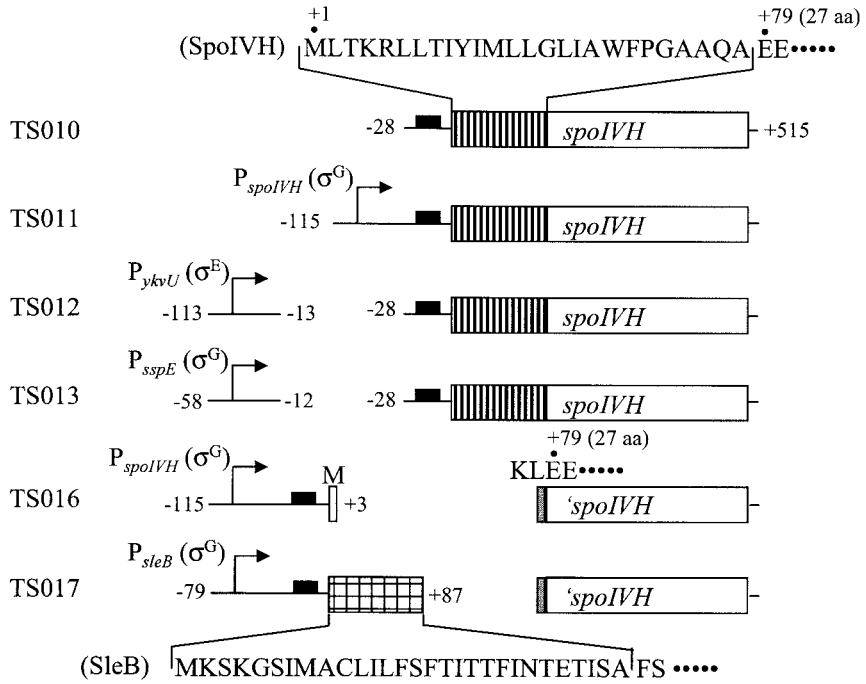

FIG. 7. Schematic representation of strains used in experiments analyzed in Tables 3 and 4. The putative Sec-type signal sequence in SpoIVH is hatched. The Sec-type signal sequence of SleB is checked. Black boxes indicate putative ribosome binding sites. Arrows with lines indicate promoters of genes and are shown to the left. *spoIVH* at the native locus was disrupted in all strains. The amino acid sequences of signal peptides and flanking regions are indicated. The peptide of KL was encoded by the HindIII restriction site (gray boxes) in TS016 and TS017. The positions of DNA fragments relative to the start codons of the original genes are indicated at the ends of the fragments.

SpoIVH-GFP strain, probably due to the low level of *spoIVH* expression. However, a peptide in the N-terminal region (1 to 26 aa) of SpoIVH closely resembles the Sec-type signals, which are involved in one of the major pathways for translocation in *B. subtilis* (45). Furthermore, the C-terminal region of the SpoIVH signal sequence contains a consensus amino acid sequence A-X-A, which serves as an SPase I cleavage site (44). The *sleB* gene, which encodes a putative spore-cortex-lytic enzyme, is translocated across the forespore inner membrane by a secretion Sec-type signal peptide and is deposited in the cortex layer synthesized between the forespore inner and outer membranes (29). To investigate the importance of the signal peptide for SpoIVH function, the region encoding the putative signal peptide (1 to 26 aa) of the SpoIVH protein was removed (TS016) or substituted (TS017) with a fragment (−79 to +87) containing the σ^G-recognized promoter region of *sleB* to the region encoding the signal peptide (1 to 29 aa) of the SleB protein (Fig. 7). As shown in Table 4, in the mutant strain without the SpoIVH signal sequence (TS016), as well as in the *spoIVH* single mutant (TS001), sporulation was inhibited, indicating that the signal sequence of SpoIVH is indispensable for SpoIVH to function efficiently. In contrast, in the other *spoIVH* mutant strain (TS017) in which the SleB signal domain replaced the signal sequence of the SpoIVH protein, the sporulation efficiency compared to that of the wild-type strain was not significantly different, indicating that the SpoIVH signal domain is functionally similar to that of the SleB protein. These results suggest that SpoIVH could act in the inner space between the double membranes where the cortex is formed.

TABLE 3. Alternative expression of *spoIVH* in mother cell or forespore[a]

Strain	Original *spoIVH*	Promoter for *spoIVH* in *thrC*	No. (CFU/ml) of:		Frequency[b]
			Viable cells	Spores	
168	Intact		2.8×10^8	2.0×10^8	0.71
TS001	Disrupted		2.0×10^8	1.3×10^4	6.5×10^{-5}
TS010	Disrupted	No promoter	1.1×10^8	1.9×10^5	1.7×10^{-3}
TS011	Disrupted	*spoIVH*	2.1×10^8	1.7×10^8	0.81
TS012	Disrupted	*ykvU* (σ^E)	1.2×10^8	1.5×10^7	0.13
TS013	Disrupted	*sspE* (σ^G)	1.8×10^8	1.7×10^8	0.94

[a] Cells were grown in DSM.
[b] Frequency is the ratio of the number of spores to that of viable cells for each strain.

TABLE 4. Sporulation by fused protein of SleB signal sequence and SpoIVH[a]

Strain	Description	No. (CFU/ml) of:		Frequency[b]
		Viable cells	Spores	
168	Wild type	2.8×10^8	2.0×10^8	0.71
TS001	*spoIVH*::pJMIVH	2.0×10^8	1.3×10^4	6.5×10^{-5}
TS016	*spoIVH*Δsignal[c]	1.0×10^8	1.5×10^4	1.5×10^{-4}
TS017	P_{sleB}-signal$_{sleB}$-*spoIVH*Δsignal[c]	2.9×10^8	1.5×10^8	0.52

[a] Cells were grown in DSM.
[b] Frequency is the ratio of the number of spores to that of viable cells for each strain.
[c] Native *spoIVH* was disrupted in strains TS016 and TS017.

DISCUSSION

Our work reveals a remarkable aspect of *spoIVH* as a gene that is expressed not only in the mother cell by $E\sigma^E$ but also in the forespore under the control of $E\sigma^G$. The strain with σ^E-directed *spoIVH* has a somewhat reduced sporulation efficiency relative to that of the strain with σ^G-directed *spoIVH*, suggesting a greater functional significance of the forespore-specific expression of *spoIVH* than that of the mother cell. However, its ability to produce a number of viable spores in either strain with the σ^E- and σ^G-directed *spoIVH* gene was 2 to 3 orders of magnitude greater than that produced by the strain with *spoIVH* lacking its promoter (Table 3). This result demonstrates that both the SpoIVH proteins produced in the forespore and the mother cell have a role in sporulation. We also showed that the SpoIVH protein possesses an irremovable N-terminal signal sequence, composed of 26 aa, but that the SpoIVH protein with a substitution of the SleB signal domain in place of its signal sequence was functional. We therefore conclude that the mature SpoIVH is primarily localized in the inner space between the double membranes where the cortex is formed.

How *spoIVH* acquired such a dual control system, however, is quite intriguing. However, *ykvU* is one of the paralogous genes of *spoVB*, with a BLAST score of 180, which is expressed by $E\sigma^E$ (35). It appears that *ykvU* may have moved to the present position from the *spoVB* region through transposition. Presumably, *spoIVH* may have acquired this transcription system under the dual control of σ^E and σ^G from the *spoVB* gene through evolution. *spoIVH* is also known to belong to the AhpC/thiol-specific antioxidant protein family (http://bacillus.genome.ad.jp/) and is paralogous to *trxA* (thioredoxin) and *resA* (thiol-disulfide oxidoreductase), with BLAST scores of 40 and 89, respectively. Proteins of this family participate in reduction and are widely conserved (3). SpoIVH may act as a thiol-specific antioxidant or thiol/disulfide bond interchange protein during sporulation. Schiott and Hederstadt (40) have reported that the CcdA protein, which is required for c-type cytochrome synthesis, is also required for the late stage of sporulation in *B. subtilis*. Erlendsson and Hederstedt (9) also speculated that CcdA is related to the role of SpoIVH. If the SpoIVH protein has a disulfide bond isomerase activity that modifies the tertiary structure of some protein(s) required for cortex formation, it may be possible that SpoIVH plays a significant role in the thiol-disulfide exchange between cysteine residues of proteins in the inner double membrane space. Among products of the many identified cortex formation genes, SpoVB, SpoVD, SpoVE, and YabQ have plural numbers of cysteine residues and membrane spanning domains, suggesting that they may be targets for SpoIVH.

In addition, it is possible that *spoIVH* is important for maintaining the redox state of some protein(s) in the space between the mother cell and the forespore. Presumably, the redox states of many proteins in the space differ relative to the mother cell and the forespore. If the SpoIVH protein has an antioxidant enzymatic activity, it may be altered to compensate for the reduction in the space between the inner and outer forespore membranes; thus, the activities of various proteins involved in spore cortex formation may be impaired in the *spoIVH* mutant. Since there is little detail on cortex formation in the space, further investigation is required to understand the activity of SpoIVH and reveal the target of SpoIVH during sporulation.

ACKNOWLEDGMENTS

We thank the Japanese and European Consortia for Functional Analysis of the *B. subtilis* Genome for providing the pMUTIN strains. We especially thank Richard Losick for providing *B. subtilis* strains, Masaya Fujita for providing the σ^K antibody, Hideaki Nanamiya, Sawako Yoshida, and Fujio Kawamura for assistance with the primer extension analysis, and Samuel Amiteye for critically reading the manuscript.

This study was supported by a grant-in-aid for scientific research on the priority area Genome Biology from the Ministry of Education, Science, Sports, and Culture of Japan.

REFERENCES

1. **Beall, B., and C. P. Moran, Jr.** 1994. Cloning and characterization of *spoVR*, a gene from *Bacillus subtilis* involved in spore cortex formation. J. Bacteriol. **176:**2003–2012.
2. **Catalano, F. A., J. Meador-Parton, D. L. Popham, and A. Driks.** 2001. Amino acids in the *Bacillus subtilis* morphogenetic protein SpoIVA with roles in spore coat and cortex formation. J. Bacteriol. **183:**1645–1654.
3. **Chae, H. Z., K. Robinson, L. B. Poole, G. Church, G. Storz, and S. G. Rhee.** 1994. Cloning and sequencing of thiol-specific antioxidant from mammalian brain: alkyl hydroperoxide reductase and thiol-specific antioxidant define a large family of antioxidant enzymes. Proc. Natl. Acad. Sci. USA **91:**7017–7021.
4. **Cutting, S., A. Driks, R. Schmidt, B. Kunkel, and R. Losick.** 1991. Forespore-specific transcription of a gene in the signal transduction pathway that governs pro-σ^K processing in *Bacillus subtilis*. Genes Dev. **5:**456–466.
5. **Cutting, S., S. Roels, and R. Losick.** 1991. Sporulation operon *spoIVF* and the characterization of mutations that uncouple mother-cell from forespore gene expression in *Bacillus subtilis*. J. Mol. Biol. **221:**1237–1256.
6. **Cutting, S., V. Oke, A. Drinks, R. Losick, S. Lu, and L. Kroos.** 1990. A forespore checkpoint for mother cell gene expression during development in *Bacillus subtilis*. Cell **62:**239–250.
7. **Dubnou, D., and R. Davidoff-Abelson.** 1971. Fate of transforming DNA following uptake by competent *Bacillus subtilis*. Formation and properties of the donor-recipient complex. J. Mol. Biol. **56:**209–221.
8. **Eichenberger, P., S. T. Jensen, E. M. Conlon, C. V. Ooij, J. Silvaggi, J.-E. Gonzalez-Pastor, M. Fujita, S. Ben-Yehuda, P. Stragier, J. S. Liu, and R. Losick.** 2003. The σ^E regulon and the identification of additional sporulation genes in *Bacillus subtilis*. J. Mol. Biol. **327:**945–972.
9. **Erlendsson, L. S., and L. Hederstedt.** 2002. Mutations in the thiol-disulfide oxidoreductases BdbC and BdbD can suppress cytochrome *c* deficiency of CcdA-defective *Bacillus subtilis* cells. J. Bacteriol. **184:**1423–1429.
10. **Errington, J.** 1993. *Bacillus subtilis* sporulation: regulation of gene expression and control of morphogenesis. Microbiol. Rev. **57:**1–33.
11. **Feucht, A., L. Evans, and J. Errington.** 2003. Identification of sporulation genes by genome-wide analysis of the σ^E regulon of *Bacillus subtilis*. Microbiology **149:**3023–3034.
12. **Fujita, M.** 2000. Temporal and selective association of multiple sigma factors with RNA polymerase during sporulation in *Bacillus subtilis*. Genes Cells **5:**79–88.
13. **Gerhardt, P., and R. E. Marquis.** 1989. Spore thermoresistance mechanisms, p. 43–63. *In* I. Smith, R. A. Slepecky, and P. Setlow (ed.), Regulation of prokaryotic development. American Society for Microbiology, Washington, D.C.
14. **Harry, E. J., K. Pogliano, and R. Losick.** 1995. Use of immunofluorescence to visualize cell-specific gene expression during sporulation in *Bacillus subtilis*. J. Bacteriol. **177:**3386–3393.
15. **Helmann, J. D., and C. P. Moran, Jr.** 2002. RNA polymerase and sigma factors, p. 289–312. *In* A. L. Sonenshein, J. H. Hock, and R. Losick (ed.), *Bacillus subtilis* and its closest relatives: from genes to cells. American Society for Microbiology, Washington, D.C.
16. **Horinouchi, S., and B. Weisblum.** 1982. Nucleotide sequence and functional map of pE194, a plasmid that specifies inducible resistance to macrolide, lincosamide, and streptogramin type B antibiotics. J. Bacteriol. **150:**804–814.
17. **Igo, M. M., and R. Losick.** 1989. Regulation of a promoter that is utilized by minor forms of RNA polymerase holoenzyme in *Bacillus subtilis*. J. Mol. Biol. **191:**615–624.
18. **Ishiwa, H., and H. Shibahara.** 1985. New shuttle vectors for *Escherichia coli* and *Bacillus subtilis*. II. Plasmid pHY300PLK, a multipurpose cloning vector with a polylinker, derived from pHY460. Jpn. J. Genet. **60:**235–243.
19. **Karow, M. L., P. Glaser, and P. J. Piggot.** 1995. Identification of a gene, spoIIR, that links the activation of σ^E to the transcriptional activity of σ^F during sporulation in *Bacillus subtilis*. Proc. Natl. Acad. Sci. USA **92:**2012–2016.

20. **Kroos, L., B. Kunkel, and R. Losick.** 1989. Switch protein alters specificity of RNA polymerase containing a compartment-specific sigma factor. Science **243:**526–529.
21. **Kunst, F., N. Ogasawara, I. Moszer, et al.** 1997. The complete genome sequence of the gram-positive bacterium *Bacillus subtilis*. Nature **390:**249–256.
22. **Lewis, P. J., S. R. Partridge, and J. Errington.** 1994. σ factors, asymmetry, and the determination of cell fate in *Bacillus subtilis*. Proc. Natl. Acad. Sci. USA **91:**3849–3853.
23. **Li, Z., and P. J. Piggot.** 2001. Development of a two-part transcription probe to determine the completeness of temporal and spatial compartmentalization of gene expression during bacterial development. Proc. Natl. Acad. Sci. USA **98:**12538–12543.
24. **Losick, R., P. Youngman, and P. J. Piggot.** 1986. Genetics of endospore formation in *Bacillus subtilis*. Annu. Rev. Genet. **20:**625–669.
25. **Losick, R., and P. Stragier.** 1992. Crisscross regulation of cell-type-specific gene expression during development in *Bacillus subtilis*. Nature **355:**601–604.
26. **Lu, S., R. Halberg, and L. Kroos.** 1990. Processing of the mother-cell σ factor, σ^K, may depend on events occurring in the forespore during *Bacillus subtilis* development. Proc. Natl. Acad. Sci. USA **87:**9722–9726.
27. **Lu, S., S. Cutting, and L. Kroos.** 1995. Sporulation protein SpoIVFB from *Bacillus subtilis* enhances processing of the sigma factor precursor Pro-σ^K in the absence of other sporulation gene products. J. Bacteriol. **177:**1082–1085.
28. **Miller, J. H.** 1972. Experiments in molecular genetics, p. 352–355. Cold Spring Harbor Laboratory, Cold Spring Harbor, N.Y.
29. **Moriyama, R., H. Fukuoka, S. Miyata, S. Kudoh, A. Hattori, S. Kozuka, Y. Yasuda, K. Tochikubo, and S. Makino.** 1999. Expression of a germination-specific amidase, SleB, of bacilli in the forespore compartment of sporulating cells and its localization on the exterior side of the cortex in dormant spores. J. Bacteriol. **181:**2373–2378.
30. **Nicholson, W. L., and P. Setlow.** 1990. Sporulation, germination and outgrowth, p. 391–450. *In* C. R. Harwood and S. M. Cutting (ed.), Molecular biological methods for *Bacillus*. Wiley, Chichester, United Kingdom.
31. **Ogasawara, N.** 2000. Systematic function analysis of *Bacillus subtilis* genes. Res. Microbiol. **151:**129–134.
32. **Partridge, K. L., J. K. Grimsley, and J. Errington.** 1993. The importance of morphological events and intercellular interactions in the regulation of re-spore-specific gene expression during sporulation in *Bacillus subtilis*. Mol. Microbiol. **8:**945–955.
33. **Perego, M.** 1993. Integrational vectors for genetic manipulation in *Bacillus subtilis*, p. 615–624. *In* A. L. Sonenshein, J. H. Hoch, and R. Losick (ed.), *Bacillus subtilis* and other gram-positive bacteria. American Society for Microbiology, Washington, D.C.
34. **Piggot, P. J., and J. G. Coote.** 1976. Genetic aspects of bacterial endospore formation. Bacteriol. Rev. **40:**908–962.
35. **Popham, D. L., and P. Stragier.** 1991. Cloning, characterization, and expression of the *spoVB* gene of *Bacillus subtilis*. J. Bacteriol. **173:**7942–7949.
36. **Ricca, E., S. Cutting, and R. Losick.** 1992. Characterization of *bofA*, a gene involved in intercompartmental regulation of pro-σ^K processing during sporulation in *Bacillus subtilis*. J. Bacteriol. **174:**3177–3184.
37. **Sambrook, J., E. F. Fritsch, and T. Maniatis.** 1989. Molecular cloning: a laboratory manual, 2nd ed. Cold Spring Harbor Laboratory, Cold Spring Harbor, N.Y.
38. **Sato, T., K. Harada, and Y. Kobayashi.** 1996. Analysis of suppressor mutations of *spoIVCA* mutations: occurrence of DNA rearrangement in the absence of a site-specific DNA recombinase SpoIVCA in *Bacillus subtilis*. J. Bacteriol. **178:**3380–3383.
39. **Schaeffer, P., J. Millet, and J. P. Aubert.** 1965. Catabolic repression of bacterial sporulation. Proc. Natl. Acad. Sci. USA **54:**704–711.
40. **Schiott, T., and L. Hederstadt.** 2000. Efficient spore synthesis in *Bacillus subtilis* depends on the CcdA protein. J. Bacteriol. **182:**2845–2854.
41. **Sterlini, J. M., and J. Mandelstam.** 1969. Commitment to sporulation on *Bacillus subtilis* and its relationship to the development of actinomycin resistance. Biochem. J. **113:**29–37.
42. **Stragier, P., and R. Losick.** 1996. Molecular genetics of sporulation in *Bacillus subtilis*. Annu. Rev. Genet. **30:**297–341.
43. **Strom, M. S., and S. Lory.** 1986. Cloning and expression of the pilin gene of *Pseudomonas aeruginosa* PAK in *Escherichia coli*. J. Bacteriol. **165:**367–372.
44. **Tjalsma, H., A. G. Stöer, A. Driks, G. Venema, S. Bron, and J. M. van Dijl.** 2000. Conserved serine and histidine residues are critical for activity of the ER-type signal peptidase SipW of *Bacillus subtilis*. J. Biol. Chem. **275:**25102–25108.
45. **Van Dijl, J. M., A. Bolhuis, H. Tjalsma, J. D. H. Jongbloed, A. D. Jone, and S. Bron.** 2002. Protein transport pathways in *Bacillus subtilis*: a genome-based road map, p. 337–355. *In* A. L. Sonenshein, J. H. Hock, and R. Losick (ed.), *Bacillus subtilis* and its closest relatives: from genes to cells. American Society for Microbiology, Washington, D.C.
46. **Wakeley, P. R., R. Dorazi, N. T. Hoa, J. R. Bowyer, and S. M. Cutting.** 2000. Proteolysis of SpoIVB is a critical determinant in signaling of pro-σ^K processing in *Bacillus subtilis*. Mol. Microbiol. **36:**1336–1348.
47. **Yanisch-Perron, C., J. Vieira, and J. Messing.** 1985. Improved M13 phage cloning vector and host strains: nucleotide sequences of the M13mp18 and pUC19 vectors. Gene **33:**103–119.